CHAPTER 5

In the preceding chapters, an attempt has been made to fully/partially replace the high SAPS containing conventional ZDDP without compromising the tribological efficiency. In the next two chapters, we are trying to give some insight on the effect of particle size, layered structures and the synergy on the tribological behaviour of nanomaterials.

With the rapid development of nanoscience and nanotechnology, nanoparticles have attracted much attention due to their unique properties and promising applications in electronics, photonics, magnetism and tribology [Astruc *et al*.(2010), Mirin *et al*.(2010), Tuysuz *et al*.(2012), Huang *et al*.(2013)]. In the field of tribology, several types of inorganic nanoparticles such as CaO, CuO, ZnO, TiO_2 and CeO_2 [Battez *et al*.(2008), Gusain *et al*.(2013), Zhang *et al*.(2011), Hu *et al*.(2000a), Battez *et al*.(2010), Bahumin *et al*.(2005)] etc. have been successfully used as antiwear and extreme pressure lubrication additives. The replacement of organic molecules by tiny nanoparticles of solid materials is not straightforward. Unfortunately the common bare inorganic nanoparticles are inherently unstable and easy to agglomerate which eventually leads to their precipitation due to gravity when added to the base oil. The main advantages of these nanoparticles over traditional additives are due to their limited tribochemical reactions since these are relatively insensitive to temperature [Battez *et al*.(2010)]. Keeping this in mind, many researchers have prepared surface-modified nanoparticles which do not agglomerate forming relatively much stable dispersions in base oil and possess pronounced application in tribological industries [Bakumin *et al*.(2005)]. Capping nanoparticles with the polar organic molecules is a convenient way to stabilize them since polar group of a capping agent interacts chemically with the surface of nanoparticles and its non-polar long alkyl chain enhances the solubility of nanoparticles in the base oil thus, improving tribological properties.

Successful use of CaO, CuO, ZnO and TiO_2 nanoparticles as lubricant additives prompted us to prepare stearic acid (SA) modified SCCZTO nanoparticles (where CCZTO represents $CaCu_{2.9}Zn_{0.1}Ti_4O_{12}$) of three different sizes 60, 80 and 90 nm and

evaluate their tribological properties. The present chapter reports therefore, investigations pertaining to testing of low SAPS SCCZTOs nanoparticles as antiwear additives in neutral paraffinic base oil under boundary lubricating conditions and characterization of the chemical film formed on the interacting metallic surfaces by X-ray Photoelectron Spectroscopy (XPS) and Energy Dispersive X-ray Spectroscopy (EDX), Scanning Electron Microscopy (SEM) and contact mode Atomic Force Microscopy (AFM).

5.1. Experimental Section

5.1.1. Chemicals

Analytical grade chemicals $Ca(NO_3)_2.4H_2O$, $Cu(NO_3)_2.3H_2O$, $(CH_3COO)_2Zn.2H_2O$, titanium dioxide, citric acid, stearic acid and absolute ethanol obtained from Merck, having high purity were used without further purification. The solvent *n*-hexane used for cleaning the specimen was obtained from Fisher Scientific Co. (Mumbai, India).

5.1.2. Synthesis of nanomaterials

5.1.2.1. Synthesis of Zn-doped CCTO (CCZTO) nanoparticles

The CCZTO nanoparticles were synthesized following the method reported earlier [Singh *et al*.(2011)] Standard solutions of metal nitrates and acetate were prepared using distilled water. Solutions of the metal nitrates in stoichiometric amount of these metallic ions were mixed in a beaker containing zinc acetate solution. Thereafter, calculated amounts of TiO_2 and citric acid equivalent to metal ions were added to the solution. The solution was heated on a hot plate using a magnetic stirrer at 70-90 ^oC to evaporate water and then dried at 100-120 ^oC in hot air oven for 12h to yield a blue gel. The gel was calcined in air at 800 ^oC for 6h in a muffle furnace to form CCZTO nanoparticles. The resultant mixture was ground into fine powder using a pestle and mortar. In order to vary particle size, the obtained CCZTO nanoparticles were further

heated at 950 ^{o}C for 6h, 8h and 12h in air abbreviated as CCZTO-6h, CCZTO-8h and CCZTO-12h, respectively.

5.1.2.2. Surface modification

Stearic acid modified CCZTO nanoparticles (SCCZTO) were synthesized from CCZTO by the procedure given below:

The CCZTO-6h nanoparticles were dispersed in 200 ml of ethanolic solution containing excess of stearic acid (SA) and refluxed at 75^{0}C for 6-8h [Zhang *et al.*(2011)]. The resultant product SCCZTO-6h was filtered, washed several times with hot ethanol and then dried in vacuum desiccator. The same protocol has been followed for CCZTO-8h and CCZTO-12h nanoparticles to obtain SCCZTO-8h and -12h nanoparticles, respectively.

5.1.3. Characterization of nanomaterials

5.1.3.1. Characterization of CCZTOs nanoparticles

5.1.3.1.1. Powder-XRD

The X-Ray diffraction patterns of CCZTOs nanoparticles synthesized by auto-combustion method are shown in Figure 5.1. X-Ray data were indexed on the basis of a cubic unit cell similar to undoped CCTO (JCPDS 75-2188) which confirm the formation of single phase. Diffraction peaks are located at 29.6°, 34.3°, 38.5°, 42.3°, 45.9°, 49.3°, 61.4° and 72.3° corresponding to the (211), (220), (013), (222), (321), (400), (422) and (440) , respectively. Absence of any peak due to zinc oxide in the XRD spectra confirmed the formation of single phase. The average crystallite size of the CCZTO-6h, CCZTO-8h and CCZTO-12h was obtained as 53, 74 and 83 nm, respectively using the Debye Scherrer formula. The average crystallite size of CCZTOs nanoparticles increased with increase in temperature.

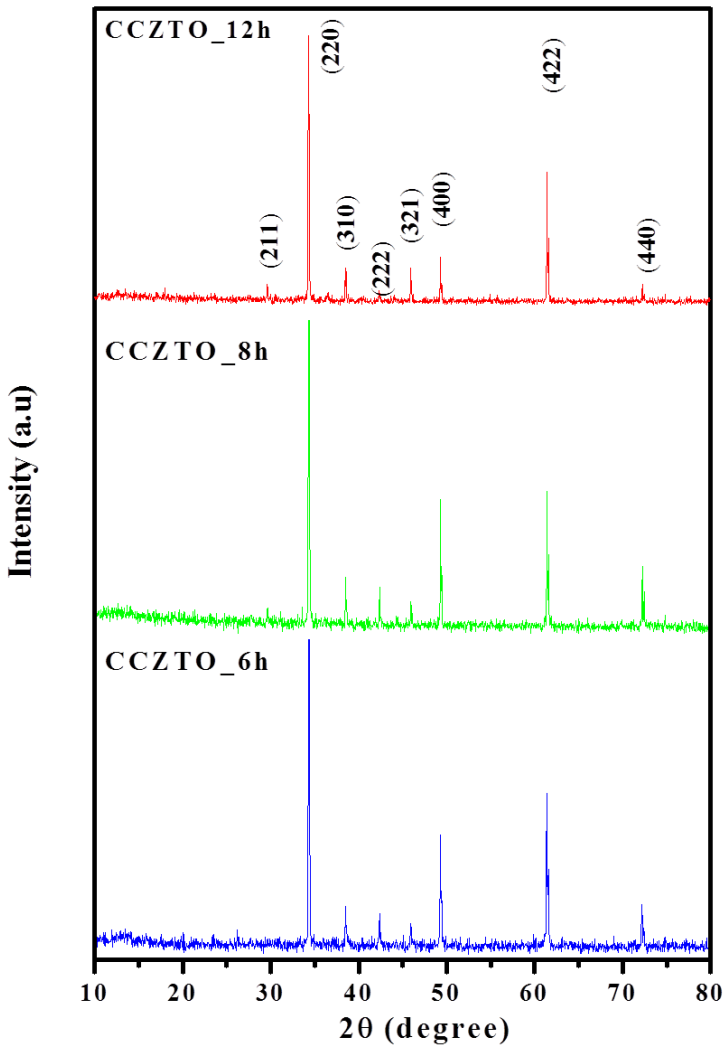

Figure 5.1. X-ray diffraction patterns of $CaCu_{2.90}Zn_{0.10}Ti_4O_{12}$ (CCZTOs) nanoparticles

5.1.3.1.2. EDX Analysis

EDX spectra of CCZTOs NPs clearly show the presence of Ca, Cu, Zn, and Ti elements as per the stoichiometric ratio and confirm the purity, Figure 5.2. The presence of zinc in the EDX spectra of CCZTOs nanoparticles also confirms the formation of Zn-doped-CCTO nanoparticles.

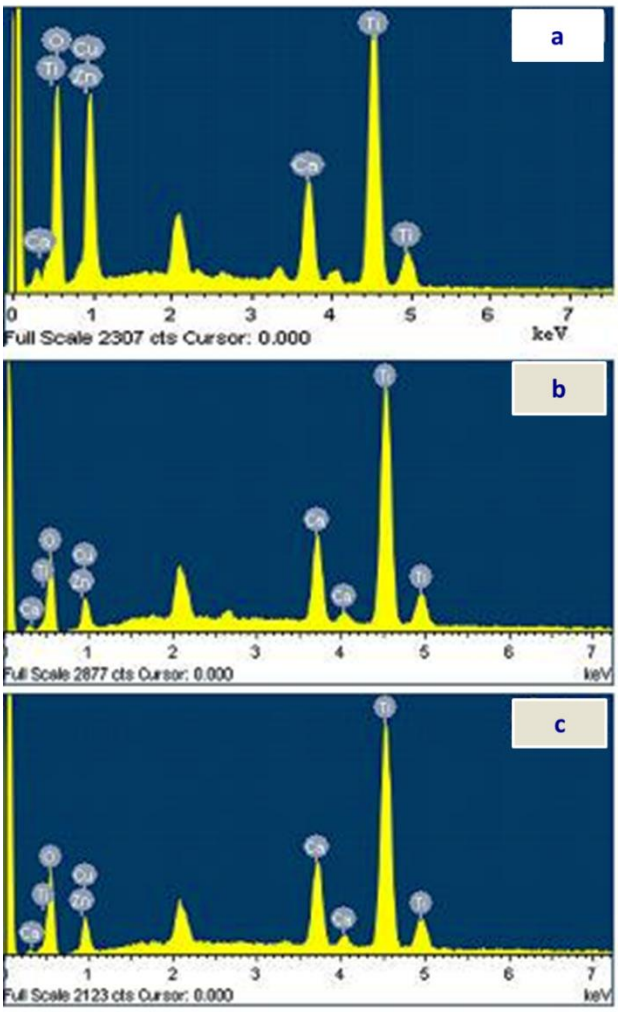

Figure 5.2. EDX spectra of $CaCu_{2.90}Zn_{0.10}Ti_4O_{12}$ (CCZTOs) nanoparticles

5.1.3.2. Characterization of SCCZTOs nanoparticles

Surface modifier agent stearic acid chemically reacts with CCZTOs nanoparticles to form surface capped SCCZTOs nanoparticles. These have been characterized by FT-IR and TEM analysis.

5.1.3.2.1. FT-IR

Figure 5.3 shows the IR spectra of CCZTO-6h, stearic acid and stearic acid modified SCCZTO-6h nanoparticles. The characteristic peak due to ν(COO) is observed around 1,710 cm^{-1} in the spectrum of stearic acid [Wang *et al.*(2006)]. This peak is completely absent in the spectrum of SCCZTO-6h, however, peaks due to $\nu(COO)_{asym}$

and ν $(COO)_{sym}$ are observed around 1,540 and 1,449 cm^{-1} respectively showing formation of stearate [Wang *et al*.(2008)]. The IR spectrum of CCZTO-6h nanoparticles shows none of the above peaks. On the basis of the observed spectra, it can be inferred that CCZTO-6h nanoparticles have been successfully modified with stearic acid to form SCCZTO-6h.

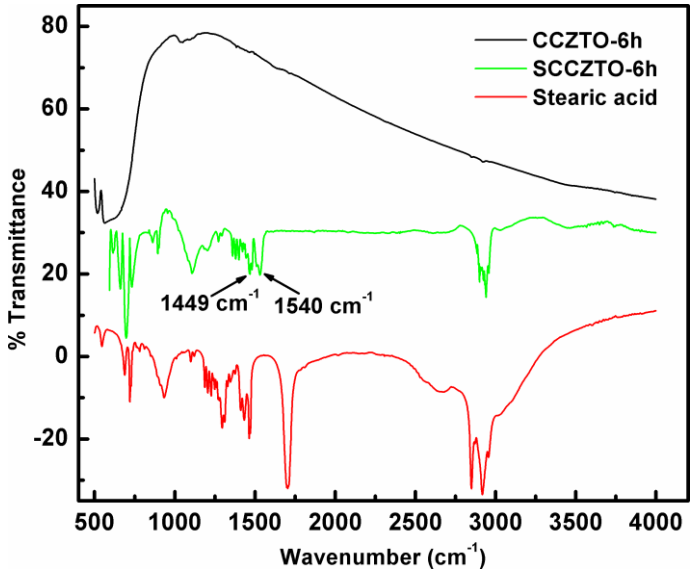

Figure 5.3. FT-IR spectra of stearic acid, CCZTO-6h and surface modified SCCZTO-6h nanoparticles

5.1.3.2.2. TEM Analysis

Transmission Electron Microscope (TEM) was used to investigate the size and agglomeration behavior of SCCZTOs nanoparticles. The dispersion of SCCZTOs nanoparticles in triple-distilled water was mounted on copper grids and examined. The TEM observations reveal that the SCCZTOs nanoparticles possess almost spherical shape and are well dispersed showing no sign of agglomeration (Figure 5.4a-c) however, in case of bare CCZTO-6h nanoparticles (Figure 5.4d), it is quite evident. Further, it can be seen from TEM-images that the average particle size of SCCZTO-6h, SCCZTO-8h and SCCZTO-12h nanoparticles is 60, 80 and 90 nm, respectively.

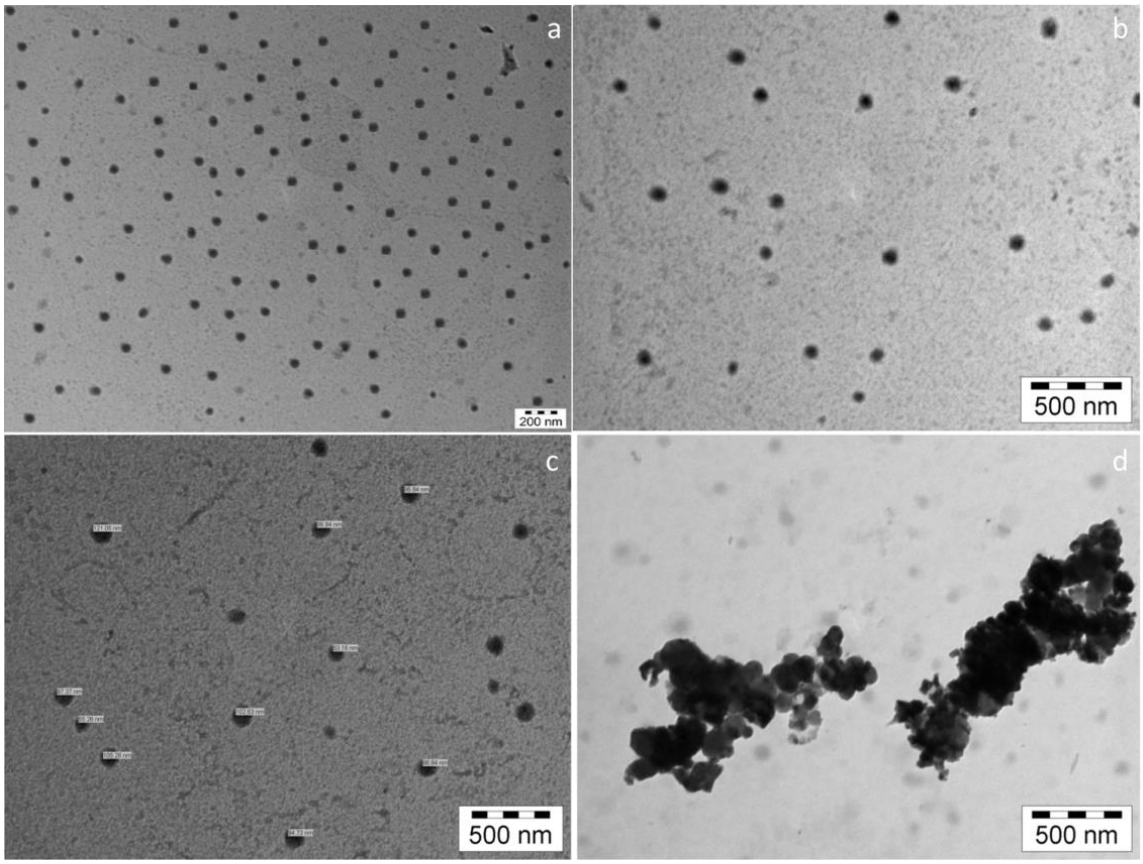

Figure 5.4. TEM images of surface-modified SCCZTOs and bare CCZTO-6h nanoparticles: **(a).** SCZTO-6h, **(b).** SCCZTO-8h **(c).** SCCZTO-12h and **(d).** CCZTO-6h nanoparticles

5.1.4. Tribological Characterization

5.1.4.1. Sample Preparation

Paraffin oil blends (uniform suspension) of SCCZTO-6h, SCCZTO-8h and SCCZTO-12h nanoparticles having concentrations 0.5, 1.0, 1.5 and 2 % (w/v) were made by stirring for 1-2h on magnetic stirrer. The entire antiwear and load carrying tests were carried out at an optimized concentration 1.0 % (w/v) of antiwear additives and compared with those of 1.0 % (w/v) ZDDP.

5.2. Results and discussion

5.2.1. Antiwear behavior

A series of friction and wear tests have been conducted to evaluate tribological properties of surface modified SCCZTOs nanoparticles. The concentration of the nanoparticles has been optimized by varying it from 0.5 to 2.0% w/v and measuring the corresponding MWD at 392N applied load for 60 min test duration. Figure 5.5 exhibits the optimization results, showing variation of MWD with change in concentration of the additives from 0.5, 1.0, 1.5 and 2.0% w/v. It can be clearly seen that the value of MWD dramatically decreases for SCCZTO-6h and SCCZTO-8h nanoparticles when their concentrations are increased from 0.5 to 2.0% w/v whereas in case of SCCZTO-12h, there is no significant reduction in MWD value. Thus the SCCZTOs, especially -6h and -8h nanoparticles improve efficiently the antiwear properties of paraffin oil at all the tested concentrations. The observed MWD values for all the additives are found to be the lowest at 1.0% w/v concentration. The SCCZTO-6h shows maximum decrease in MWD at all the concentrations followed by -8h and then -12h nanoparticles. As distinct from the Figure, beyond the optimum concentration of additives, the MWD is negligibly increased to a constant value. Therefore, all the tests were carried out at 1% w/v, the optimized concentration of the additives.

In order to investigate the effect of test duration on the mean wear scar diameter, the antiwear tests have been carried out at 392N applied load for 15, 30, 45, 60, 75 and 90 min time durations using paraffin oil in presence and absence of antiwear additives. The variation of MWD with respect to time duration at 392N load is represented in Figure 5.6. It is evident from the Figure 5.6 that the MWD, in case of paraffin oil for all the test durations is found to be much larger than in presence of the additives. In every case, MWD in the presence of SCCZTOs nanoparticles and ZDDP have been found to be much lower than the base oil. Initially, for 15 min of test duration the value of MWD in

the presence of SCCZTO-6h nanoparticles and ZDDP is found to be nearly the same, increasing slightly in case of -8h but appreciably for -12h nanoparticles. Further increase in test duration up to 30 min, there is increase in MWD in every case but slope of curve is almost equal for SCCZTO-6h, -8h while it is larger in case of -12h nanoparticles but approximately matching with that of ZDDP. Further, up to 75 min test runs, MWD for all the additives increases slightly though the rate of increase is very low. Beyond 75 min, MWD approaches to almost constant value usually for all the additives except ZDDP where a sudden increase in its value is observed. Among all the tested additives, the value of MWD for SCCZTO-6h was found to be the lowest for all test durations from 15 min to 90 min.

Initially, there is no tribofilm on the interacting surfaces. As the time increases the additive molecules get uniformly distributed over the mating surfaces during sliding under operating conditions (high load and high temperature) and may react with metal surface to form tribochemical film. The formation of tribofilm is time dependent; therefore, some time exposure is required to form a durable tribofilm on sliding surfaces [Fuller *et al*.(1997)]. During 15 min test, the tribofilm formation on the interacting surfaces could not get initiated consequently large values of MWD are observed in every case. The constant values of the MWD thereafter, suggest the existence of some tribofilm on the surface. The additive molecules are adsorbed on the surface through stearate. The order of observed antiwear behavior shown by the studied nanoparticles is in accordance with the size of nanoparticles; smaller the size of nanoparticles, better are the antiwear properties. It may be due to the fact that the smaller nanoparticles may easily fill in the valleys of metallic surfaces thus preventing direct metal-metal contact. It might be one of the reasons behind the observed trend of additives in the present investigation.

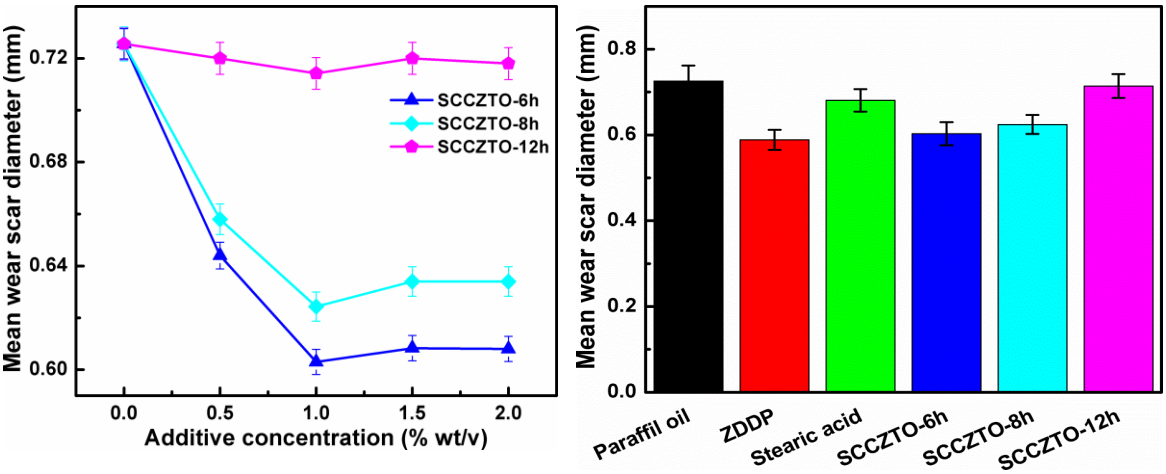

Figure 5.5. Variation of mean wear scar diameter in absence and presence of different concentrations of SCCZTOs nanoparticles in paraffin oil at 392N applied load and 60 min duration

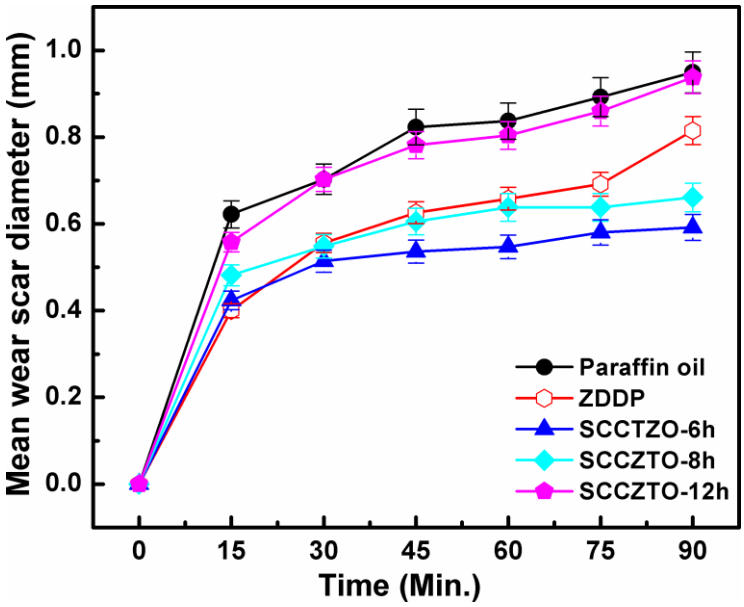

Figure 5.6. Variation of mean wear scar diameter with time in paraffin oil containing (1% w/v) zinc dibutyldithiophosphate and SCCZTOs nanoparticles at 392N applied load

The dependence of friction coefficient (μ) on time duration in absence and presence of 1% w/v ZDDP/SCCZTOs nanoparticles in paraffin oil for 392N applied load is shown in Figure 5.7. It can be seen that the blends of base oil with SCCZTO-6h and -8h give the lower friction coefficient than that with ZDDP or -12h nanoparticles. In

general, values of μ for all the additives increase initially up to 30 min test run and then decrease slightly or remain constant up to 75 min duration. As discussed above, formation of protective tribofilm prior to 30 min run, in fact, is not complete rather just initiated. Further increase in time duration up to 90 min results in increase of μ values in general and ZDDP, in particular. This may due to the wear assisted surface damage and generation of wear debris produced with time under operating conditions at the interface [Verma *et al*.(2008)]. The friction coefficient curve of SCCZTO-12h shows entirely different behavior. The friction coefficient increases steadily up to 45 min time duration, the increase in its value becomes smaller up to 75 min time duration but becomes abrupt after that up to 90 min test run. The poorest antiwear activity exhibited by SCCZTO-12h can be explained on its largest particle size which does not allow the nanoparticles to traverse through valleys of interacting surfaces restricting their movement.

On the basis of variation of mean wear scar diameter and friction coefficient with time the order of antiwear efficiency is given below:

SCCZTO-6h > SCCZTO-8h > ZDDP > SCCZTO-12h > Paraffin oil

To estimate wear more realistically it is important to examine the variation of mean wear volume with time instead of variation of mean wear scar diameter with time. Mean wear volume in absence and presence of different additives at 392N load for paraffin oil was plotted as a function of time and a linear regression model was fitted on the points including origin to find out overall wear rate, Figure 5.8. Overall wear rate was found to be very high in absence of additives. Among all the three SCCZTOs nanoparticles, the following order has emerged for overall wear rate:-

SCCZTO-6h < SCCZTO-8h < SCCZTO-12h

This again is in conformity with the conclusion drawn earlier that owing to smaller size, SCCZTO-6h efficiently smoothen the surface irregularities forming stronger tribofilm thus reducing wear to the greatest extent.

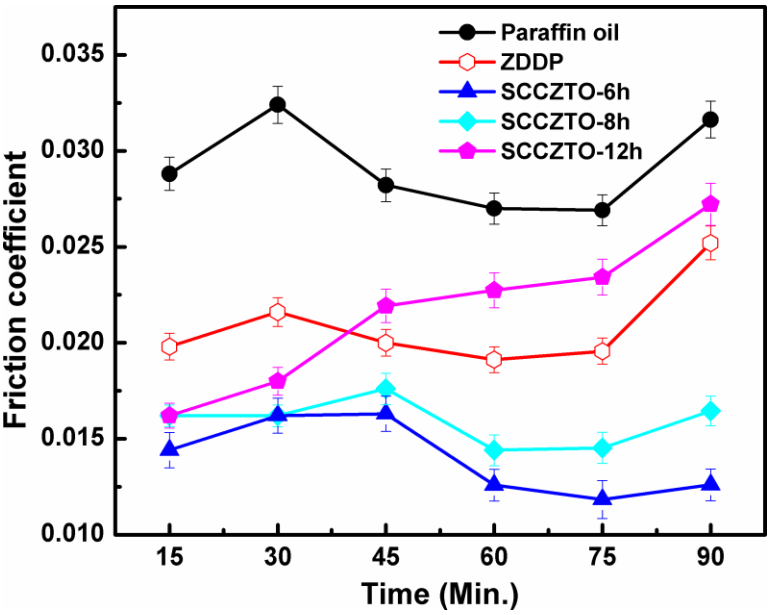

Figure 5.7. Variation of friction coefficient with time in paraffin oil containing (1% w/v) zinc dibutyldithiophosphate and SCCZTOs nanoparticles at 392N applied load

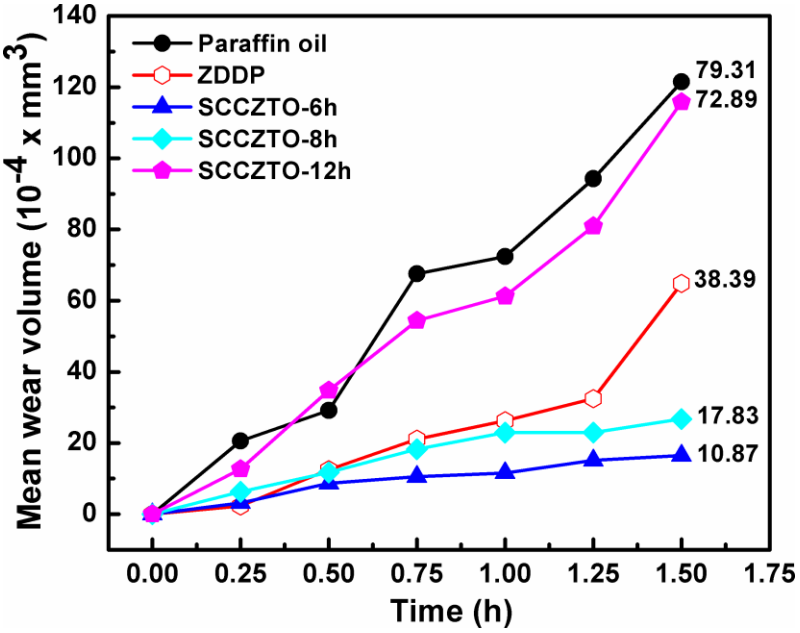

Figure 5.8. Determination of overall wear rate by varying mean wear volume with time in paraffin oil containing (1% w/v) zinc dibutyldithiophosphate and SCCZTOs nanoparticles at 392N applied load

The running-in wear rate is always higher than the steady-state wear rate as it involves morphological modifications of the surfaces. The values of overall, running-in and steady-state wear rate are listed in Table 5.1. Table shows that the running-in wear rate is found to be lower in case of SCCZTO-6h and SCCZTO-8h than ZDDP while the steady-state wear rate in their presence is much lower than ZDDP. The life of engineering components is estimated on the basis of steady-state wear rate. Thus, for a better antiwear additive it is important to achieve steady-state as early as possible and it must be stable for longer duration. The addition of SCCZTOs nanoparticles to the paraffin base oil effectively reduces the overall, running-in and steady-state wear rates.

Table 5.1. Wear-rate for paraffin oil in the presence and absence of different SCCZTO nanoparticles and ZDDP (1%w/v) for 90 minute test duration at 392 N applied load.

S.N.	Lubricants	Wear rate (10^{-4} x mm^3/h)		
		Overall	Running-in	Steady-state
1	Paraffin oil	79.31	84.48	53.52
2	SCCZTO-6h	10.87	14.82	09.15
3	SCCZTO-8h	17.83	24.06	09.40
4	SCCZTO-12h	72.89	74.08	50.22
5	ZDDP	38.39	29.41	22.78

5.2.2. Effect of load

In order to investigate the effect of applied load on the mean wear scar diameter, the tests have been carried out at different loads 294, 392, 490, 588 and 686N for 30 min test duration for paraffin oil in presence and absence of SCCZTOs nanoparticles (1% w/v). Figure 5.9 represents plots of MWD as a function of applied load at 30 min test duration. It can be clearly shown from the Figure that paraffin oil, stearic acid and ZDDP could sustain the load up to only 490 and 588N respectively whereas SCCZTOs nanoparticles reflect appreciable load carrying ability up to 686N.

At initial load (294N), MWD is very large in the absence of additives but in presence of SCCZTOs nanoparticles it is fairly reduced. At 392N load, MWD increases appreciably in every case but this increase is maximum in absence of additives. This shows that the thin film of lubricant and additive adsorbed on the interacting surfaces resists much increase in MWD on increasing applied load. At 490N load the base oil, stearic acid show abrupt increase in MWD; however, the increase is very small in presence of the nanoparticles. This can be attributed to the formation of tribofilm in presence of SCCZTOs nanoparticles. Thus, the tribofilm formed is further capable of carrying higher load. Beyond 490N load the tribofilm fails to sustain the load in case of paraffin oil while the film fails at 588N load in case of blends with ZDDP. On further increase in the applied load up to 686N, SCCZTOs nanoparticles could successfully bear the load without surface destruction. This is one of the most striking features of the investigated SCCZTOs nanoparticles.

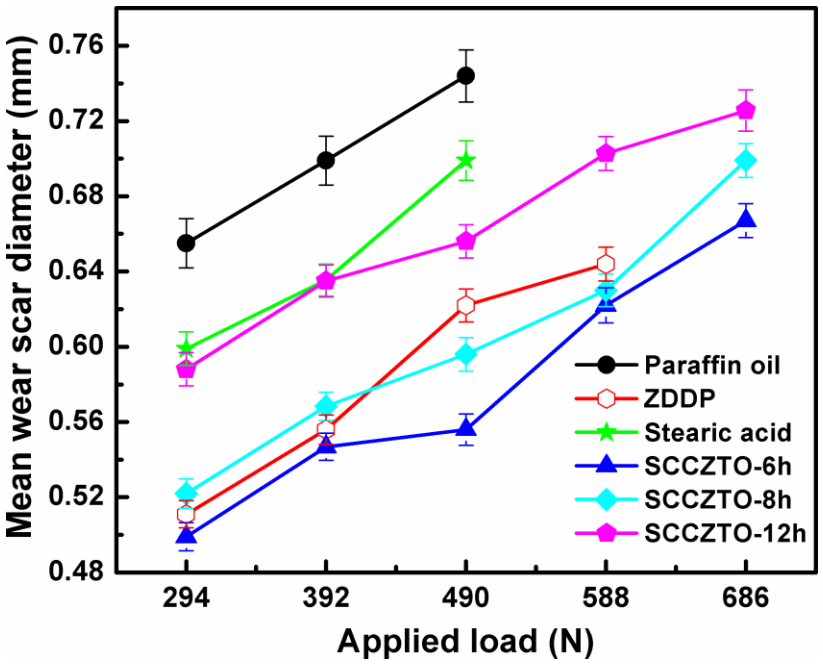

Figure 5.9. Variation of mean wear scar diameter with applied load in paraffin oil containing (1% w/v) zinc dibutyldithiophosphate and SCCZTOs nanoparticles for 30 min test duration

5.2.3. Surface characterization

5.2.3.1. Surface Morphology

The surface topography of the worn surfaces has been studied by scanning electron microscopy (SEM) and Atomic Force Microscopy (AFM). SEM micrographs of the wear scar in the presence and absence of 1% SCCZTOs nanoparticles at the applied load 392N and 90 minute duration are shown in Figure 5.10(a-e). The surfaces in presence of additives are smoother as compared to that lubricated with paraffin oil alone (Figure 5.10a) where huge surface destruction indicating a severe wear is observed. This surface damage is obviously reduced when the SCCZTOs nanoparticles are mixed with the base oil causing wear process to slow down. The SEM micrographs of steel balls lubricated with SCCZTO-6h (Figure 5.10b) and SCCZTO-8h (Figure 5.10c) nanoparticles at different magnifications show much smoother surface as compared to those obtained with ZDDP (Figure 5.10d) in which some wider grooves were observed. Moreover, in case of surface lubricated with SCCZTO-12h (Figure 5.10e) nanoparticles shows the wear debris adhered on the surface of wear track. The observed smoothness of micrographs in presence of new additives follows the same order as inferred on the basis of their tribological behavior discussed above.

To investigate the morphology of worn steel surfaces lubricated with SCCZTO-6h nanoparticles and ZDDP at comparatively higher load, the SEM micrographs have been also taken at 588N load for 30 min test duration. These micrographs are presented in Figure 5.11. It can be clearly seen from the Figure 11a, that much more surface damage is observed in case of ZDDP, on the contrary, relatively much smoother surface has been obtained when SCCZTO-6h nanoparticles Figure 11b are used.

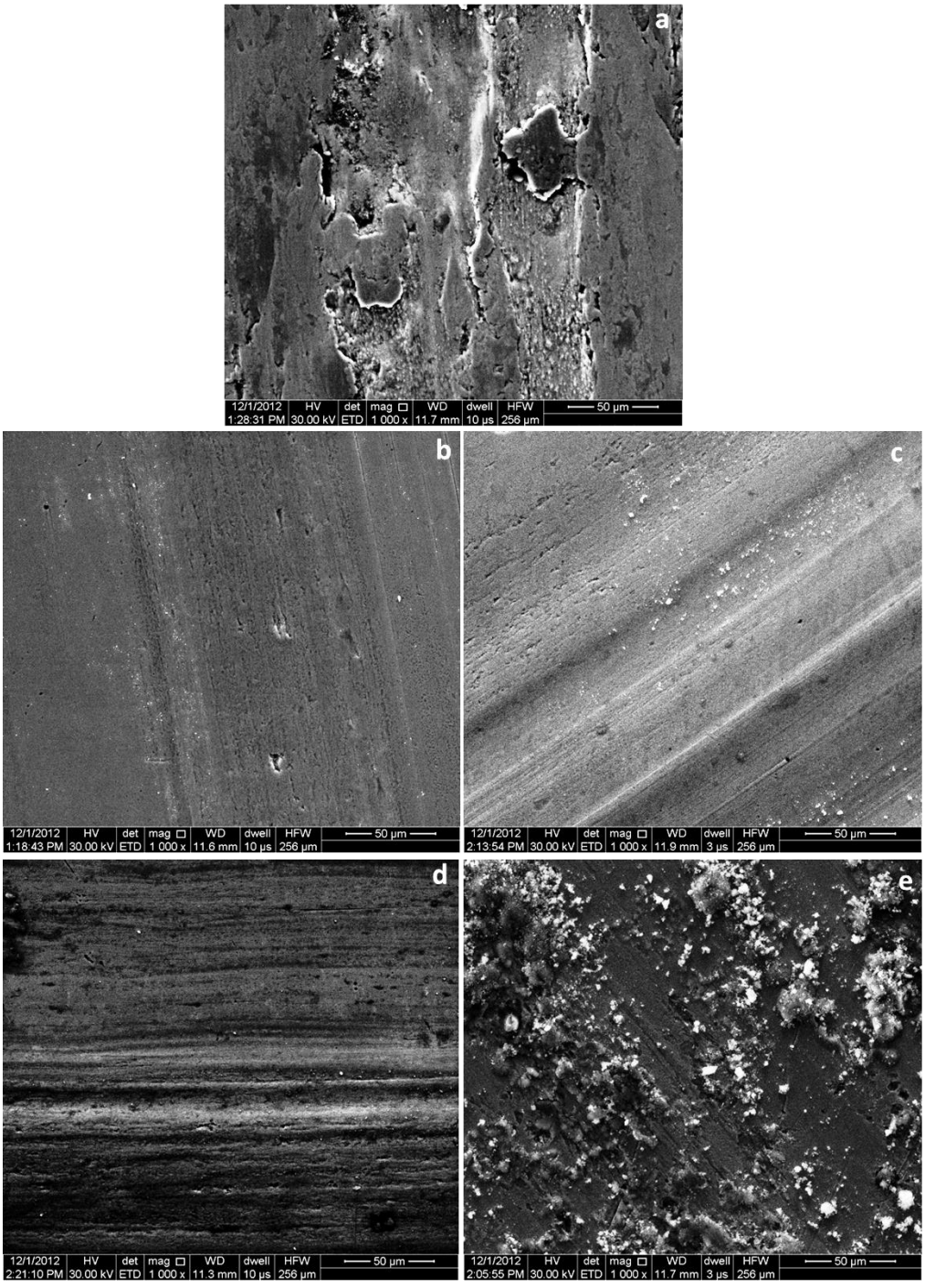

Figure 5.10. SEM micrographs of the worn steel surface lubricated with different additives (1% w/v) in paraffin oil for 90 min test duration at 392N applied load: (a) Paraffin oil, (b) SCCZTO-6h, (c) SCCZTO-8h, (d) ZDDP and (e) SCCZTO-12h

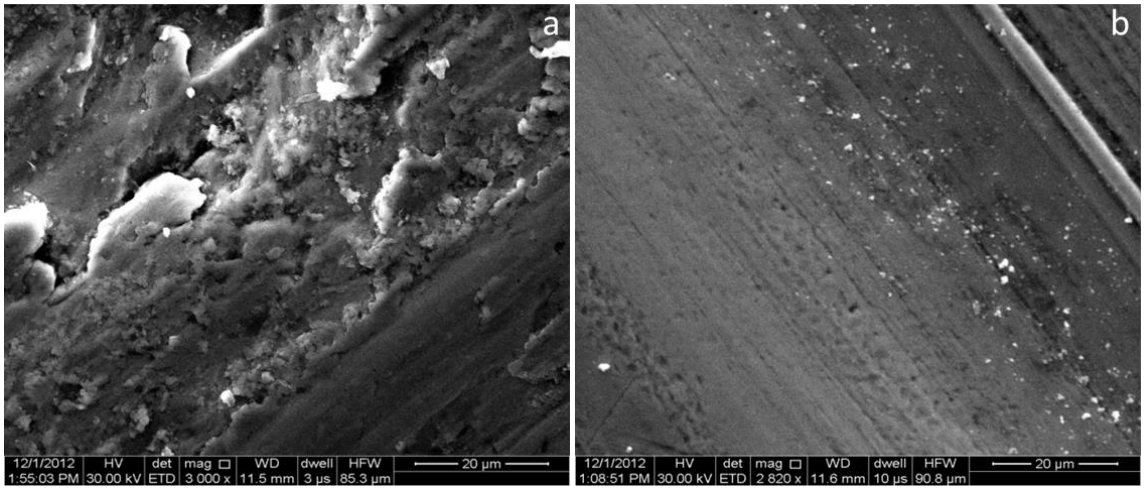

Figure 5.11. SEM micrographs of the worn steel surface lubricated with (a) ZDDP and (b) SCCZTO-6h nanoparticles (1% w/v) in paraffin oil for 30 min test duration at 588N applied load

Surface topography of the worn surfaces on the steel balls observed after antiwear testing at load 392N for 90 min test duration in paraffin oil, was studied by Atomic Force Microscopy in absence and presence of the SCCZTOs nanoparticles and ZDDP. The AFM images of the worn surfaces are shown in Figure 5.12(a-e). On comparing the *2D* and *3D*-AFM images of wear track lubricated with paraffin oil, ZDDP, SCCZTO-6h, -8h and -12h nanoparticles (Figure 5.12a-e); it clearly reflects that the spherical nanoparticles uniformly adhere and/or tribosintered during the sliding conditions owing to their excellent tribological behavior. Among all of the SCCZTOs nanoparticles, degree of compactness has been found to be maximum in case of smaller sized (60nm) nanoparticles i.e. SCCZTO-6h followed by -8h (80nm) and then -12h (90nm). From these figures it can be also inferred that the relative order of the nanoparticles size is in accordance with the experimentally found size by TEM. As the size of nanoparticles increases, their efficiency towards antiwear behavior decreases. The large projections are seen in case of paraffin oil alone whereas in case of additives, the asperities of relatively much smaller dimension are observed. Among all of the SCCZTOs nanoparticles and ZDDP, wear track lubricated with SCCZTO-6h nanoparticles shows tremendous

reduction in both surface roughness and average asperities height. The value of area roughness has been found to be maximum, 409nm (Sq) for the base oil and minimum, 48nm (Sq) for SCCZTO-6h. As apparent from these figures, the roughness has fairly reduced in the presence of nanoparticles. The maximum reduction of surface roughness has been observed in case of SCCZTO-6h (Sq=48nm) which indeed, is much better than that in case of ZDDP (Sq=75nm) under similar conditions. The reduction in surface roughness may be attributed to the tribofilm formed under test conditions by the nanoparticles.

5.2.3.2. Tribochemistry of SCCZTOs nanoparticles

The EDX spectra of the worn surface lubricated with paraffin oil and its suspension with ZDDP and SCCZTO-6h nanoparticles have been recorded to determine the elemental compositions of the tribofilm at 392N load for 90 min test duration, Figure 5.13. Figure 5.13a exhibits the EDX spectrum of the worn steel surface lubricated with paraffin oil alone. It does not show any peak due to hetero atoms except oxygen which may be due to the oxide formation. On the other hand, Figure 5.13b shows prominent additional peaks for zinc, phosphorous, sulfur and nitrogen on the wear scar surface lubricated with additive ZDDP. The percentage atomic contents of the worn surface lubricated with base oil, ZDDP and SCCZTO-6h nanoparticles are listed in Table 5.2. The EDX spectrum of wear scar surface lubricated with SCCZTO-6h nanoparticles, Figure 5.13c shows presence of calcium, copper, zinc, titanium, iron and oxygen on the worn surface. In order to investigate the tribochemical interaction of SCCZTO-6h nanoparticles, the EDX spectrum (Figure 5.14) has also been taken at a higher load, 588N, for 30 min duration and its results are mentioned in Table 5.3. It is evident from Table 5.3 that the atomic concentration of different elements increases appreciably with increase in load in case of SCCZTO-6h nanoparticles while its reverse is observed in case of ZDDP. This contrast may be due to the strengthening of tribofilm in the former case while its rupture in the latter one.

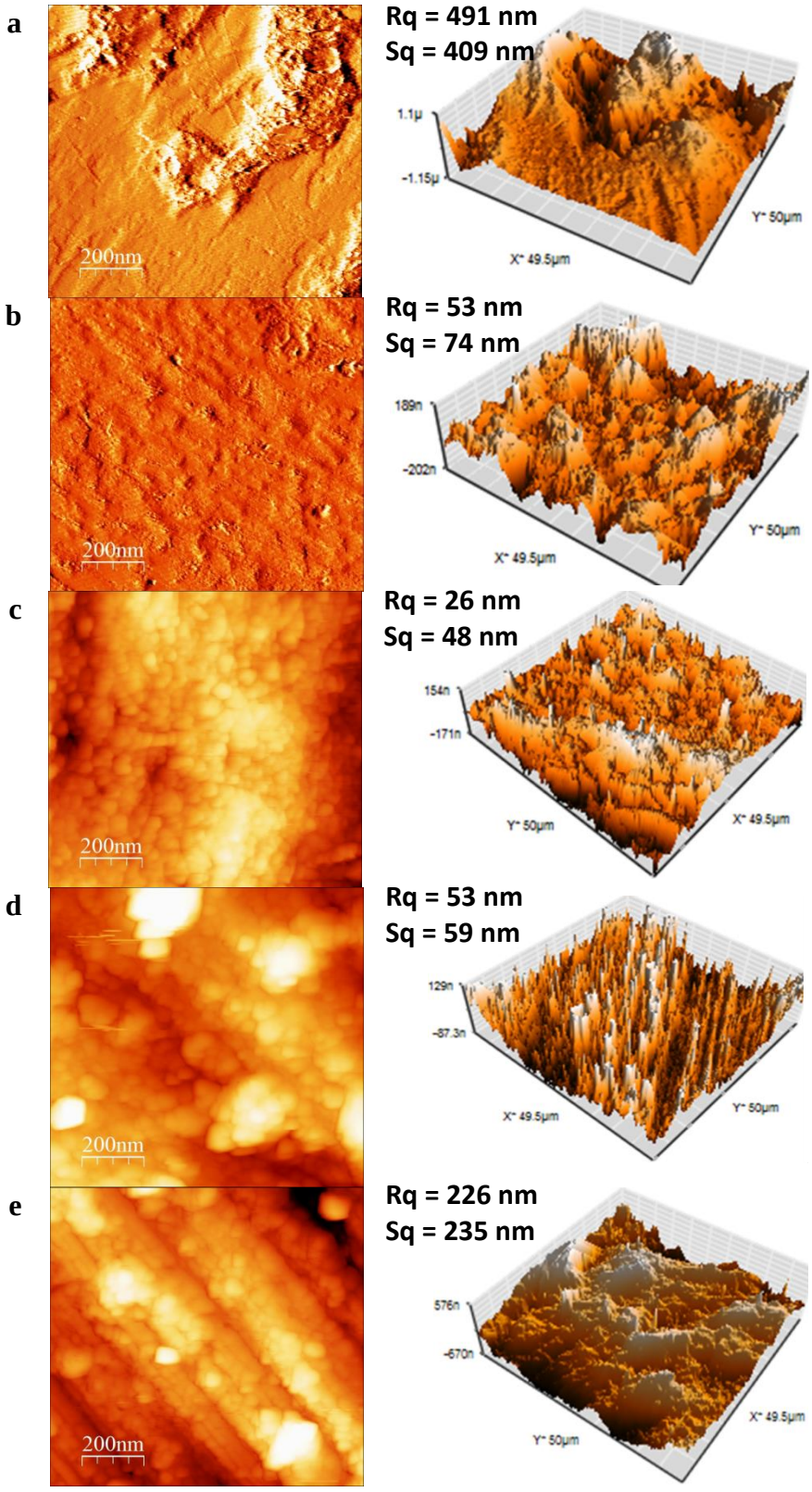
a
Rq = 491 nm
Sq = 409 nm
1.1µ
-1.15µ
Y= 50µm
X= 49.5µm
200nm
b
Rq = 53 nm
Sq = 74 nm
189n
-202n
Y= 50µm
X= 49.5µm
200nm
c
Rq = 26 nm
Sq = 48 nm
154n
-171n
Y= 50µm
X= 49.5µm
200nm
d
Rq = 53 nm
Sq = 59 nm
129n
-87.3n
X= 49.5µm
Y= 50µm
200nm
e
Rq = 226 nm
Sq = 235 nm
576n
-670n
Y= 50µm
X= 49.5µm
200nm

Figure 5.12. 2*D* and *3D* AFM images of the worn steel surface with and without SCCZTOs nanoparticles (1% w/v) in paraffin oil for 90 min test duration at 392N applied load: (a) Paraffin oil, (b) Zinc dibutyldithiophosphate, (c) SCCZTO-6h, (d) SCCZTO-8h and (e) SCCZTO-12h

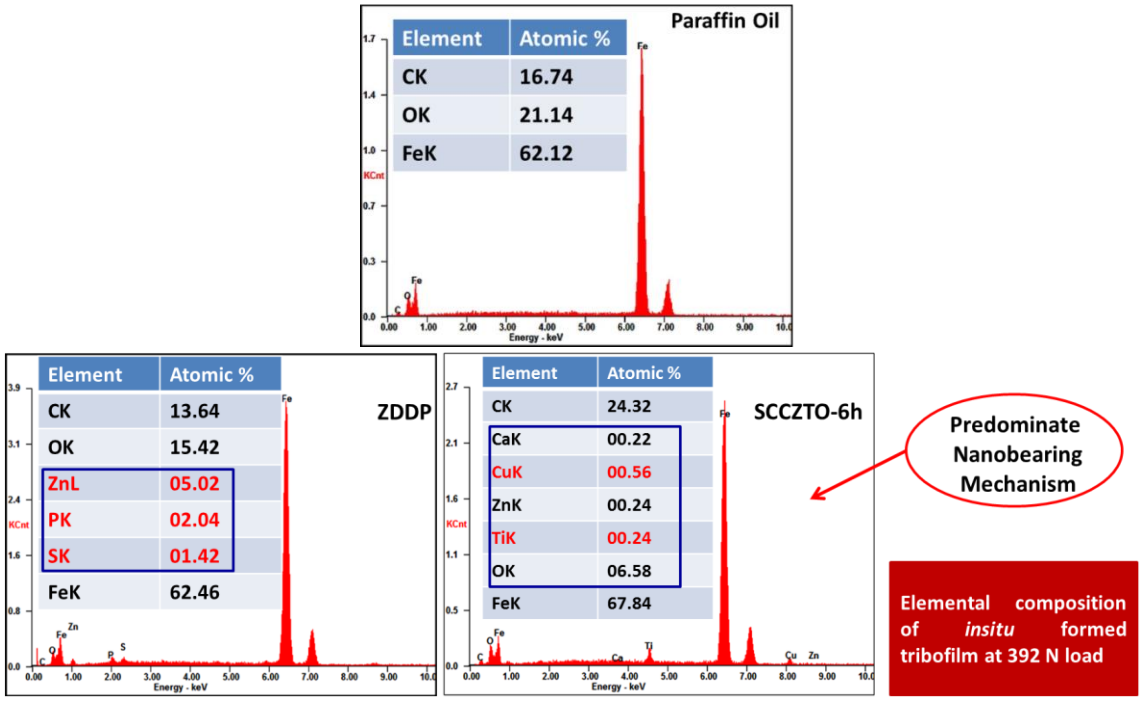

Figure 5.13. EDX analysis data of the worn steel surface lubricated with paraffin oil in presence and absence of additives (1% w/v) for 90 min test duration at 392N applied load: (a) Paraffin oil, (b) Zinc dibutyldithiophosphate (ZDDP) and (c) SCCZTO-6h

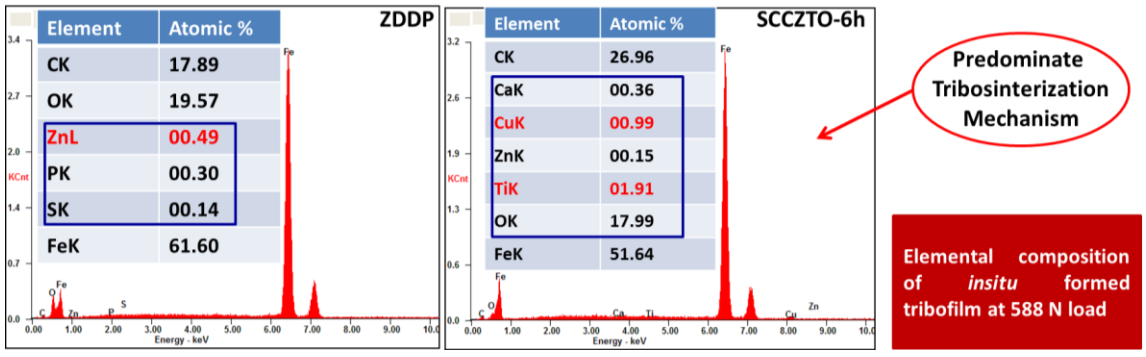

Figure 5.14. EDX analysis data of the worn steel surface lubricated with paraffin oil in presence of additives (1% w/v) for 30 min test duration at 588N applied load: (a) Zinc dibutyldithiophosphate (ZDDP) and (b) SCCZTO-6h

Table 5.2. EDX analysis data of the worn steel surface under lubricating condition with and without additives for 90 minute duration at 392 N applied load: (a). Paraffin oil; (b). ZDDP (1% w/v) and (c). SCCZTO-6h nanoparticles **(**1% w/v)

a.

Element	Atomic %
CK	16.74
OK	21.14
FeK	62.12

b.

Element	Atomic %
CK	13.64
OK	15.42
ZnL	05.02
PK	02.04
SK	01.42
FeK	62.46

c.

Element	Atomic %
CK	24.32
CaK	00.22
CuK	00.56
ZnK	00.24
TiK	00.24
FeK	67.84
OK	06.58

Table 5.3. EDX analysis data of the worn steel surface lubricated with additives in paraffin oil for 30 min test duration at 588 N applied load: (a). ZDDP (1% w/v) (b). SCCZTO-6h nanoparticles **(**1% w/v)

(a).

Element	Atomic %
CK	17.89
OK	19.57
ZnL	00.49
PK	00.30
SK	00.14
FeK	61.60

(b).

Element	Atomic %
CK	26.96
CaK	00.36
CuK	00.99
ZnK	00.15
TiK	01.91
FeK	51.64
OK	17.99

The detailed chemical analysis of tribofilm on worn surfaces has been studied using XPS. XPS analysis of the worn scar in presence of the blend with SCCZTO-6h at 392N load for 90 min test duration was carried out. Figure 5.15(a-f) shows the XPS spectra of C 1s, Ca 2p, Cu 2p, Ti 2p, O 1s and Fe 2p of the wear scar.

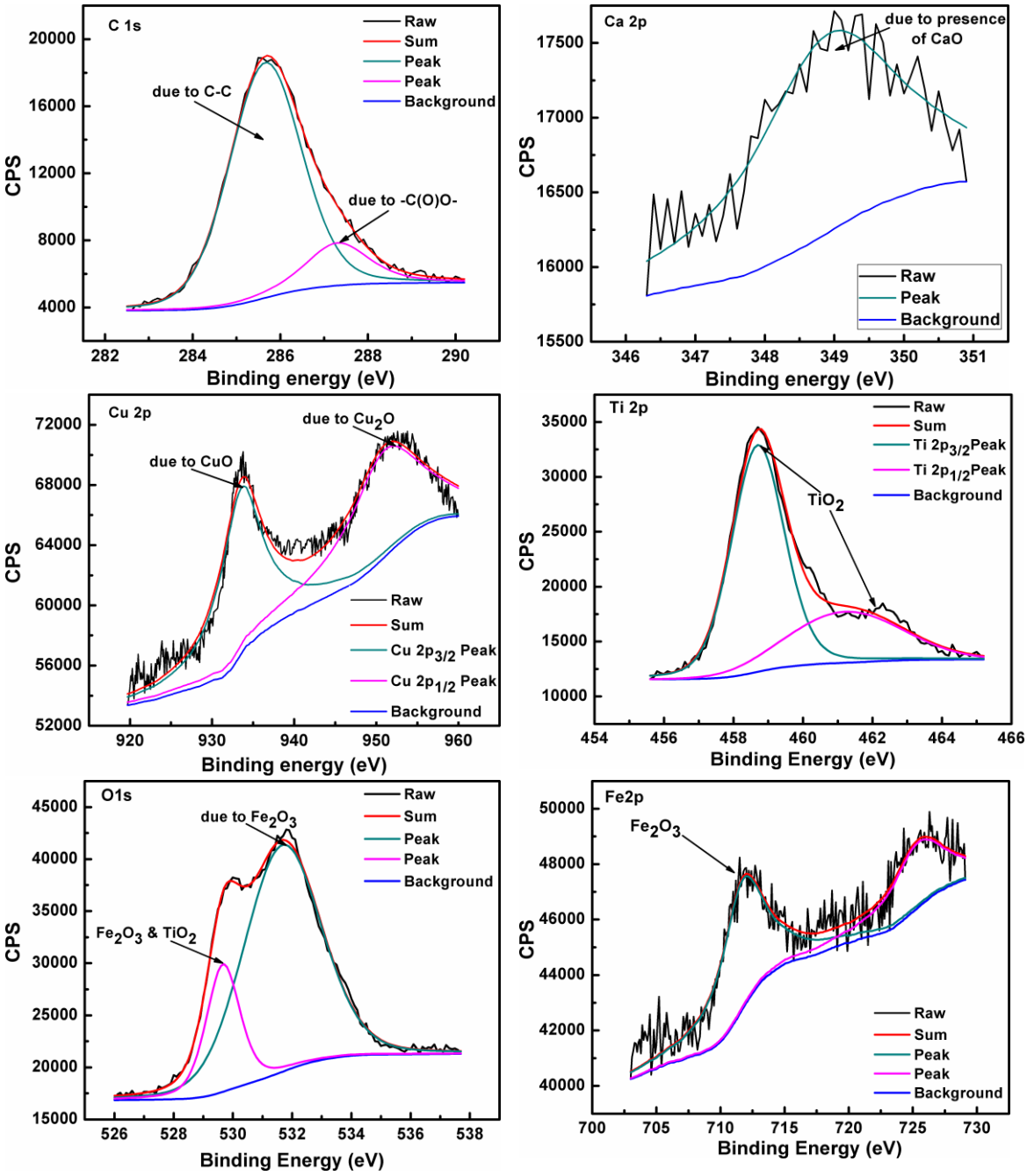

Figure 5.15. XPS spectra of tribochemical film formed on worn steel surface lubricated with SCCZTO-6h nanoparticles (1% w/v) at 392N applied load for 90 min test duration in liquid paraffin. (a). C 1s, (b). Ca 2p, (c). Cu 2p, (d). Ti 2p, (e). O 1s, and (f). Fe 2p

The spectrum of C 1s on the worn surface exhibits peaks at 285.8 and 287.4 eV corresponding to -C(O)O- and C-C/C-H moieties respectively, which may be attributed to presence of stearate moiety [Wang *et al.*(2006)]. The weak signal of Ca 2p appearing at

about 349.2 eV, indicates the presence of CaO on the worn surface [Zeng *et al*.(2007)]. The spectrum of Cu 2p on worn surface illustrates the existence of two peaks at 933.84 and 952.2 eV due to Cu $2p_{3/2}$ and Cu $2p_{1/2}$ respectively showing occurrence of both CuO and Cu_2O. The presence of CuO is expected, as CuO is one of the constituent of SCCZTO nanoparticles while formation of Cu_2O is probably due to the partial reduction of Cu(II) because of its interaction with surface or the other constituents [Battez *et al*.(2010)]. The binding energies of Ti 2p have been found to be 458.6 and 462.3 eV corresponding to Ti $2p_{3/2}$ and Ti $2p_{1/2}$ respectively due to the presence of TiO_2 [Xue *et al*.(1997)]. Furthermore, on combining the binding energy of O 1s with Ti 2p, the peak at 529.8 eV confirms the presence of TiO_2 on the worn surfaces. Combining the binding energies of Fe 2p at 711.2 eV with O 1s at 531.8 eV, it can be stated that iron has oxidized to Fe_2O_3 during rubbing process [Li *et al*.(2006)]. The major constituents of SCCZTO-6h nanoparticles are stearate moiety, CaO, CuO, ZnO and TiO_2. The presence of all these constituents (except ZnO) on the worn surface lubricated with SCCZTO-6h nanoparticles confirms the process of tribosinterisation under operating conditions which is responsible for their lubricating behavior.

5.2.4. Proposed mechanism for antiwear behavior

It is well known that all the metallic surfaces are not smooth and contain numerous asperities and valleys. In case of mixed or boundary lubricating conditions when the lubricant film between the tribo-pairs becomes thinner, the additive may carry a proportion of load and separate the two surfaces to prevent adhesion [Li *et al*.(2006)]. The stearate of the SCCZTOs nanoparticles reacts with metal surface at mild load or lower time duration to form a chemical film as evident from the observed XPS spectra. The antiwear mechanism of the investigated additives may follow three different processes: (i) the nanoparticles may melt, get welded on the shearing surfaces and react with sliding surfaces to form tribofilm, (ii) or these may act as a third body on shearing surfaces i.e. like nano-bearings and (iii) or these may get tribosintered on the surfaces [Battez *et al*.(2010)]. In case of SCCZTOs nanoparticles, the first proposed mechanism seems to be not applicable as their melting points are beyond 2000^0C, their melting and

welding to form a tribofilm can be easily ruled out. The additives may follow the second proposed mechanism where thermally stable metal oxides having spherical shape may act as nano-bearings and carry the load. In case, the nanoparticles are acting as nano-bearings, these should have been washed away during surface preparation for XPS and EDX. On the contrary, EDX data (Tables 5.2c and 5.3b) and XPS spectra (Figure 5.15) show the presence of atomic contents of the additive on the surface indicating that nanoparticles are not merely acting as nano-bearings. In the third option, tribosinterisation, the nanoparticles get deposited in the valleys surrounded by asperities under high pressure and temperature and form more compact tribofilm which prevents direct metal to metal contact showing outstanding tribological behavior. Therefore, the additives with smaller size easily traverse through valleys and act as excellent wear reducing agents. In our case, the atomic concentration at the surface has increased considerably when load is increased from 392N to 588N which is evident from EDX spectral data, Tables 5.2c and 5.3b. This shows that at lower load/smaller time duration, inorganic nanoparticles appear to follow nano-bearing as well as tribosinterisation mechanisms, however, at higher loads or greater time durations these follow tribosinterisation process to form a strong tribofilm and thereby reducing wear.

5.3. Conclusions

The stearic acid capped nanoparticles could be well dispersed without agglomeration in paraffin oil. These blends effectively enhanced the antiwear properties of base oil in order of decreasing particle size. The overall, running-in and steady-state wear rates of SCCZTOs nanoparticles except -12h have been found to be lower than ZDDP. The load bearing ability of the SCCZTOs nanoparticles was found to be far better than ZDDP and paraffin oil alone. Surface analysis by SEM and AFM also supports the observed tribological behavior of SCCZTOs nanoparticles. The EDX analysis of wear track shows presence of C, Ca, Cu, Zn, Ti, O and Fe elements in the tribofilm whereas XPS spectra revealed chemical form of these elements as -C(O)O-, C-C/C-H moieties; CaO; CuO, Cu_2O; TiO_2 and Fe_2O_3. EDX and XPS analysis support the mechanism of wear through nanobearing as well as process of tribosinterisation.